



Manchester Metropolitan University

García-Escárzaga, A and Clarke, LJ and Gutiérrez-Zugasti, I and González-Morales, MR and Martínez, M and López-Higuera, JM and Cobo, A (2018) *Mg/Ca profiles within archaeological mollusc (*Patella vulgata*) shells: Laser-Induced Breakdown Spectroscopy compared to Inductively Coupled Plasma-Optical Emission Spectrometry*. *Spectrochimica Acta Part B: Atomic Spectroscopy*, 148. pp. 8-15. ISSN 0584-8547

Downloaded from: <http://e-space.mmu.ac.uk/620903/>

Publisher: Elsevier

DOI: <https://doi.org/10.1016/j.sab.2018.05.026>

Usage rights: Creative Commons: Attribution-Noncommercial-No Derivative Works 4.0

Please cite the published version

<https://e-space.mmu.ac.uk>

1 **Mg/Ca profiles within archaeological mollusc (*Patella vulgata*) shells: Laser-Induced**
2 **Breakdown Spectroscopy compared to Inductively Coupled Plasma-Optical Emission**
3 **Spectrometry**

4

5 Asier García-Escárcaga^{1,2}; Leon J. Clarke³; Igor Gutiérrez-Zugasti¹; Manuel R. González-
6 Morales¹; Marina Martínez²; José-Miguel López-Higuera²; Adolfo Cobo^{2*}

7

8 ¹ Instituto Internacional de Investigaciones Prehistóricas de Cantabria, Universidad de
9 Cantabria. Edificio Interfacultativo, Avda. Los Castros s/n. 39005 Santander, España.

10 ² Grupo de Ingeniería Fotónica, Departamento de TEISA, Universidad de Cantabria, Edificio
11 I+D+i de Telecomunicaciones, Avda. Los Castros s/n. 39005 Santander, Spain.

12 ³ School of Science and the Environment, Faculty of Science and Engineering, Manchester
13 Metropolitan University, Manchester, M1 5GD, UK.

14 *Corresponding author.

15

16 Email addresses:

17 a.garcia.escarzaga@gmail.com (A. García-Escárcaga), l.clarke@mmu.ac.uk (L.J. Clarke),
18 igorgutierrez.zug@gmail.com (I. Gutiérrez-Zugasti), moralesm@unican.es (M.R. González-
19 Morales), marina.martinez@unican.es (M. Martínez), miguel.lopezhiguera@unican.es (J.M.
20 López-Higuera); adolfo.cobo@unican.es (A. Cobo).

21

22 **Abstract**

23 Biogenic carbonate mollusc shells have the unique property of being a durable material found
24 in many archaeological and geological sites, recording in their shell chemical composition the
25 ambient environmental conditions during the mollusc's lifespan. In particular, mollusc shell
26 Mg/Ca ratios have been suggested to be related to seawater temperature, although such a
27 relationship is controversial and appears to be species- and even location-specific. This study
28 investigates the use of Laser-Induced Breakdown Spectroscopy (LIBS) for the rapid

1 measurement of Mg/Ca profiles within *Patella vulgata* shells, via comparison with one
2 established analytical technique that is most often used for this purpose, ICP-OES. LIBS offers
3 some advantages over other spectrometric techniques, including ICP-OES, the latter requiring
4 initial micromilling of sample powders. LIBS offers faster measurement, reduced sample
5 preparation, easier automation and less complex and lower cost instrumentation. A high
6 correlation is evident between LIBS and ICP-OES Mg/Ca profiles within four archaeological
7 *P. vulgata* shells, as well as strong similarities between LIBS measurements made in two
8 different areas of each *P. vulgata* shell (i.e. the apex and a more conventional transect along
9 the axis of shell growth). Validation of the LIBS technique for determination of Mg/Ca profiles
10 within *P. vulgata* shells has implications for archaeological studies, because a greater number
11 of shell specimens sampled from each archaeological site and chronological level can be
12 measured, thereby improving the statistical robustness of data interpretation and conclusions.
13 One example archaeological application that would benefit from application of the LIBS
14 technique is identification of the season-of-capture of marine molluscs as a food resource for
15 prehistoric societies.

16

17 **Key words:** Mollusc shells, Mesolithic, LIBS, ICP-OES, Mg/Ca profiles, Season-of-capture,
18 Paleoclimatology

19

20 **1. Introduction**

21

22 Marine mollusc shells are routinely found in many geological [1] and archaeological deposits
23 [2], from low to high latitudes [3]. They can preserve valuable information about past climate
24 conditions, because their chemical composition (i.e. a chemical proxy) during the growth of
25 the shell can be dependent on the ambient environmental conditions, in particular seawater
26 temperature. One potential seawater temperature proxy is the amount of, minor elements (e.g.
27 magnesium and strontium) that substitute for calcium within the crystal structure of the mollusc
28 shell carbonate mineral [6]. These elemental analyses are most frequently performed using
29 spectrometry techniques such as Inductively Coupled Plasma-Optical Emission Spectroscopy
30 (ICP-OES), Inductively Coupled Plasma-Mass Spectroscopy (ICP-MS) and also Laser
31 Ablation Inductively Coupled Plasma- Mass Spectroscopy (LA-ICP-MS) [6-8]. All of these

1 ICP-based analytical techniques facilitate measurement of the molar concentrations of each
2 element incorporated into the mollusc shell carbonate. In contrast, Laser-Induced Breakdown
3 Spectroscopy (LIBS) has been much less frequently used for determinations of mollusc shell
4 elemental concentrations [9-12]. One of the main advantages of LIBS, compared to ICP-based
5 techniques, is the reduction in the time required to perform spatially-resolved analyses, because
6 LIBS does not require extensive sample preparation [13]; LA-ICP-MS also is considerably
7 more costly and complex instrumentation [14, 15].

8 The relationship between mollusc shell elemental ratios and seawater temperature is, however,
9 still somewhat controversial. Only a few studies have identified a strong dependence of mollusc
10 shell Mg/Ca on seawater temperature, and secondary factors, such as growth rate, or even
11 location, also can influence elemental incorporation [16-20]. Therefore, additional studies are
12 required on different mollusc species, in order to determine whether their shell Mg/Ca ratios
13 can be applied to archaeological investigations and past climate reconstructions. The LIBS
14 methodology, and associated substantial reduction in analytical time [21], potentially could be
15 applied to increase the number of mollusc shell specimens that can be studied. To that end, the
16 LIBS technique would be particularly useful in archaeological studies seeking to determine
17 mollusc season-of-capture, i.e. at what time of the year this marine food resource was harvested
18 by prehistoric societies, for which a large number of mollusc shells need to be measured in
19 order to obtain statistically significant results. Similarly, LIBS could well have future potential
20 for enhancing palaeoclimatological applications, when measurement of a larger number of
21 specimens would also increase the robustness of past climate change reconstructions.

22 In this study, Mg/Ca ratios in four archaeological shells of *Patella vulgata* Linnaeus, 1758
23 (common limpet) collected from archaeological shell middens from the Cantabrian region
24 (northern Iberia) have been measured with LIBS, for two different parts of the shell, and
25 compared for the first time (for this biogenic carbonate material) with the established ICP-OES
26 technique. The advantages and limitations of using LIBS for applications of the type described
27 here, specifically with archaeological implications, are discussed.

28

29 **2. Materials and Methods**

30

31 **2.1. Archaeological shells**

1 Four *P. vulgata* specimens were collected from the archaeological shell midden site of El
2 Mazo, located in the town of Andrín, near Llanes, Asturias, northern Spain. The majority of
3 this archaeological assemblage is assigned to the Mesolithic chronological period, approx. 10
4 700–6 800 calibrated radiocarbon years before present (BP), a period during which marine
5 molluscs were an important food resource [22]. The specimens analysed in this study were
6 recovered from four different stratigraphic units (numbered 107, 105, 112 and 101) and dated
7 as Early Holocene, from 8 400 cal years BP to 7 900 cal years before present (see [9]).

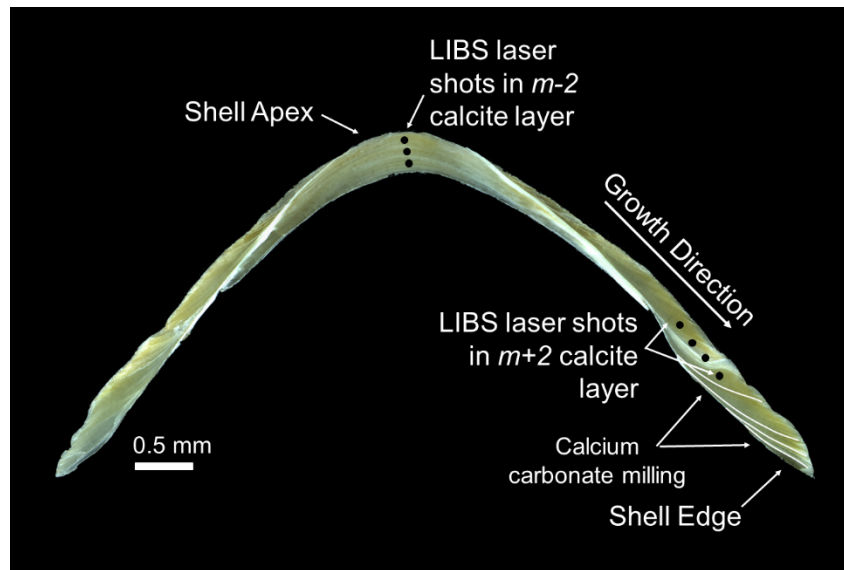
8

9

10 **2.2. ICP-OES sample preparation and determination of intra-shell Mg/Ca profiles**

11 The four *P. vulgata* shells studied were first cleaned using ultrapure water and air-dried at
12 ambient laboratory temperature. Subsequently, each shell specimen was partially coated with
13 a metal epoxy resin along the axis of maximum growth, i.e. from anterior to posterior margins,
14 to avoid the shell breaking when it was sectioned along the main growth axis. Sectioning was
15 performed using a Buehler Isomet low-speed saw and a diamond wheel. The thick (~1.5 mm)
16 sections obtained then were fixed onto a glass microscope slide with metal epoxy resin and
17 polished, using 1 µm diamond suspension grit, until the internal growth lines and increments
18 were clearly visible (Fig. 1). For ICP-OES element/Ca determinations, calcium carbonate
19 powder samples were milled from the $m+2$ calcite layer [25], using a New Wave MicroMill
20 and a 1 mm drill bit, samples being removed sequentially every 100 to 200 µm following the
21 growth direction from the shell edge. These samples always weighed more than 100 µg. All
22 powder samples were placed in acid-cleaned 1.5 ml micro-centrifuge tubes immediately after
23 milling.

24



1

2 Fig. 1: Thick-section of *P. vulgata* specimen MA.105.3 showing where the CaCO_3 powder samples were micromilled for ICP-
 3 OES measurements, as well as the sampling path for the LIBS measurements near the shell apex ($m-2$ layer) and along the
 4 $m+2$ calcite layer [25]. Powder samples were removed sequentially from the shell edge, along the growth direction axis, using
 5 a MicroMill and a 1 mm drill bit. White lines show the powder micromilling sampling strategy and black dots are an illustration
 6 of the path of the LIBS laser shots (actual craters are smaller and more closely spaced)

7 Each milled powder sample was then dissolved in 1 ml of 0.075 M HNO_3 (Ultrapure grade)
 8 inside the 1.5 ml micro-centrifuge tubes. Micro-centrifuge tubes were placed into an ultrasonic
 9 bath for 15 minutes and then left overnight. The next day, samples were centrifuged for 5
 10 minutes at 1 500 rpm to collect any insoluble residue in the base of the tubes, the upper 0.8 ml
 11 of the 0.075 M HNO_3 digest solution being removed and added to 2.2 ml of 0.075 M HNO_3 in
 12 13 ml autosampler tubes. Mg/Ca ratios were determined using a Thermo Scientific iCAP6300
 13 ICP-OES at Manchester Metropolitan University (UK), using emission line wavelengths 317.9
 14 nm for Ca and 279.5 nm for Mg.

15 An intensity-ratio calibration was applied for ICP-OES elemental ratio determinations [26],
 16 using synthetic standard solutions in the range 0 to 35 mmol/mol for Mg/Ca. Elemental ratio
 17 calibration standards were prepared and measured at Ca concentrations ranging between 5 and
 18 40 $\mu\text{g/ml}$ (in 5 $\mu\text{g/ml}$ increments), with sample Ca concentrations then matched to the closest
 19 calibration standard to minimise any Ca matrix effect on Mg/Ca ratios. ICP-OES analytical
 20 precision was monitored by running intermediate elemental ratio calibration standards every 5
 21 to 6 samples. On the four days of analysis, Mg/Ca precision (expressed as %RSD; N = 31, 30,
 22 26 and 25) was 0.70%, 0.42%, 0.93% and 0.71%. In order to determine the accuracy and
 23 precision of ICP-OES sample Mg/Ca determinations, and to facilitate correction of subtle
 24 differences among different days of analysis, two certified reference materials (CRMs) were
 25 measured, i.e. ECRM-752 and CMSI-1767 [27, 28]. For each CRM, approximately 50 mg was

1 dissolved in 50 ml of 0.075M HNO₃, before being diluted to a nominal Ca concentration of 15
2 µg/ml (1.875 ml of each CRM stock solution made up to 50 ml with 0.075m HNO₃). Analysis
3 of the CRMs, distributed within ICP-OES sample sequences, returned a precision (expressed
4 as %RSD; N = 13, 6, 12 and 10; total N = 41) of 1.83% for all Mg/Ca measurements, also
5 yielding a Mg/Ca accuracy within 99.2% of reported values [28].

6

7 **2.3. LIBS set-up and intra-shell Mg/Ca profiles**

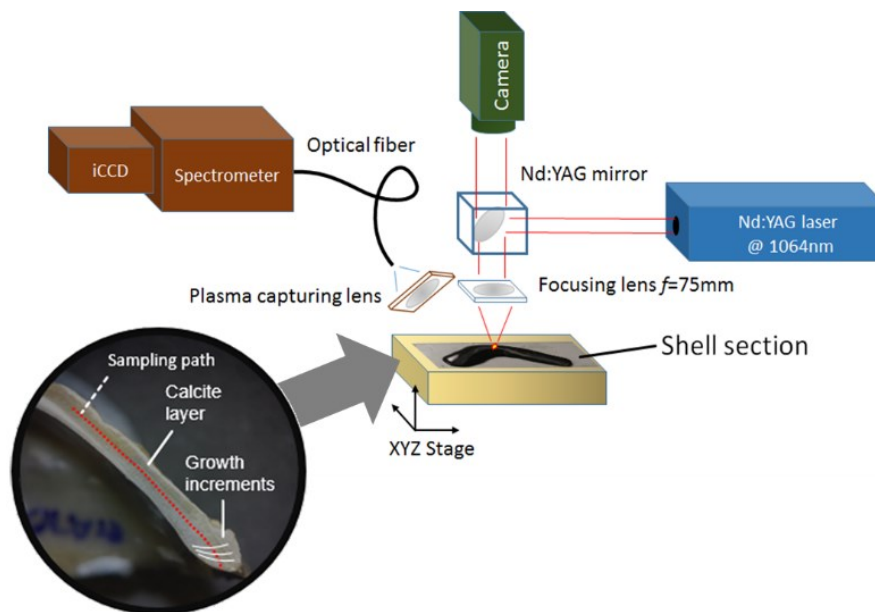
8 The same four *P. vulgata* shell samples were measured using a LIBS setup after micromilling
9 of powders for ICP-OES measurements, without any further sample preparation. The
10 automated measurement setup is shown in Fig. 2. The laser source is a Q-Switched Nd:YAG
11 (Lotis LS-2147) emitting 16 ns pulses at 1 064 nm with a 10 Hz repetition rate and 35 mJ of
12 energy per pulse. The laser beam was focused on the sample with a 75 mm focal fused-silica
13 lens. The light from the generated plasma at the sample surface was captured by a 600 µm-
14 diameter optical fibre coupled to an Acton SP-300i spectrometer with a Princeton Instruments
15 PIMAX-3 intensified CCD detector. The spectrometer was configured with a capture window
16 of 20 µs, starting 0.5 µs after the laser shot, a compromise value that results in a low
17 contribution of the background radiation but strong atomic emission lines. Arranged co-axially
18 with the focusing optics, an industrial-grade colour CCD camera enabled visual observation
19 and recording of a small area (7x5 mm) of the sample surface around the focal point of the
20 laser. The sample was placed on an XYZ motorised stage that enables a precise path to be
21 followed across the shell section and real-time correction of the focal position to account for
22 surface height irregularities. All aspects of the LIBS set-up are controlled by custom software
23 in Matlab[®], which allows a user to draw a sampling path across the mollusc shell surface to
24 follow the specimen's maximum growth axis.

25 The measurements were performed in two different areas of *P. vulgata* shell cross-sections:

26 (1) Sampling paths followed the centre of calcite layer $m+2$ (after [25]; see Fig. 1), starting
27 from the shell edges (i.e. the most recently deposited material). This is the same shell layer
28 from where material for ICP-OES analyses was previously micromilled (it is also the part of
29 the shell on which oxygen-isotope ratio analyses are typically performed [29]). The distance
30 between LIBS sampling points was fixed at 200 µm and the crater size was 100 µm in diameter,
31 with no overlap. 50 laser shots were fired at every sampling point to improve the signal to noise
32 ratio of the generated optical spectra.

1 (2) Linear paths from the exterior of the shell's apex to the inner surface of the shells (area in
2 contact with the mollusc), through the inner calcite layer $m-2$ (see Fig. 1). This area has only
3 recently been explored for determination of elemental ratios using the LA-ICP-MS technique
4 [30]; in this part of the *Patella* limpet shell the growth increments are “compressed” into a
5 small thickness of only $\sim 1-2$ mm, compared to the 10s of millimetres that span all of the
6 growths increments within the $m+2$ layer. Classical analytical techniques that require
7 micromilling of sample powders (ICP-OES, ICP-MS and IRMS) cannot achieve sufficient
8 spatial resolution in the apex region of these marine mollusc shells. LIBS measurements in this
9 $m-2$ layer have been performed every $25 \mu\text{m}$, with ca. $75 \mu\text{m}$ overlap between individual
10 measurements. In the biogenic calcite with crossed-foliated matrix that forms both $m+2$ and
11 $m-2$ layers, the LIBS ablation process in this setup produces circular craters $100 \mu\text{m}$ in diameter
12 with an average depth of $0.2 \mu\text{m}$ per laser shot.

13



14

15 Fig. 2: LIBS experimental setup including a Nd:YAG pulsed laser, Zerny-turner spectrometer with iCCD, through-lens
16 camera and a XYZ motorized stage for the sample.

17

18 Mg/Ca ratios were determined from LIBS emission spectra. First, one emission peak for each
19 element was selected: 285.2 nm for Mg and 300.7 nm for Ca. These are different emission lines
20 to the ones used for ICP-OES measurements (279.5 nm for Mg and 317.9 nm for Ca) in order
21 to obtain peaks with more similar heights and closer wavelengths [31]. These lines have been
22 verified to be not saturated and free from self-absorption. Then, the ratio of the integrated area

1 of the two emission peaks was calculated for every spectrum, and the average ratio (of 50
2 spectra) was obtained at each LIBS measurement point. Some of the LIBS experiments
3 undertaken in this study have been performed with the spectrometer configured with a “wide”
4 low resolution spectral window, from 277 to 563 nm, using a 150 grooves/mm grating, while
5 others employed a “narrow” spectral window, from 274 to 306 nm, using a 1200 grooves/mm
6 grating. The wide window enables processing of different emission lines of the same elements,
7 as well as investigation of the presence (or not) of other elements (e.g. Sr, Li and Ba) within
8 the carbonate matrix, but could result in saturated spectra due to the many strong calcium
9 emission lines that are sampled. The narrow window can be focused on selected emission lines
10 with higher signal to noise ratio and no saturation.

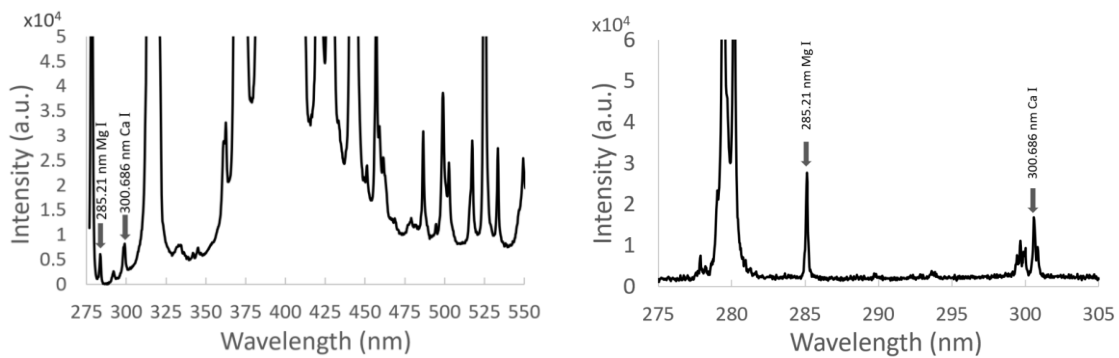
11 In order to verify the validity of the selected analytical lines (i.e. a linear relationship between
12 the Mg/Ca molar ratio and the calculated LIBS raw intensity ratio), a custom reference material
13 with similar composition to the marine biogenic carbonates and with known Mg/Ca ratios
14 (from 0.2% to 10%) was created (as reported in [9]). The results obtained showed a clear linear
15 correlation ($R^2= 0.99$) with the actual Mg/Ca molar ratio for a wide range of concentrations (2
16 mmol/mol to 100 mmol/mol), thus confirming the suitability of the LIBS configuration and
17 selection of emission lines described here for this application. Using the expression
18 recommended by [32], a Limit of Detection (LoD) value of 0.122 mmol/mol was found for the
19 wide spectral window and 0.043 mmol/mol for the narrow window [9]. The data derived from
20 this study suggest a LIBS analytical precision (expressed as %RSD; N=50 per reference
21 material) of 2.24%.

22 Because the captured LIBS spectra are not corrected for the wavelength-dependent optical
23 efficiency of the experimental setup, and due to the absence of specific matrix-matched
24 calibration standards for the marine mollusc shell biogenic carbonate measured, the resulting
25 LIBS Mg/Ca is a raw value expressed in arbitrary units (a.u.), unlike the ICP-OES derived
26 molar concentration units (i.e. mmol/mol). Furthermore, the Mg/Ca values (a.u.) measured by
27 LIBS are consistently representative of the actual Mg/Ca molar ratio only when the LIBS
28 experimental conditions (e.g. gain intensifier, optical alignment or spectrometer configuration)
29 are identical between data collection intervals, a situation that was not always possible during
30 this study. Different normalization approaches [32] and calibration-free LIBS (CF-LIBS)
31 techniques [33] have been tested to address this limitation, but the results are unreliable due to
32 limitations of the LIBS instrumental set-up applied in this study; for the narrow spectral
33 window the number of spectral lines is too low, while for the wide window the spectral

1 resolution is not high enough. The current LIBS instrumental configuration used in this work
2 prevents accurate values of the plasma temperature and electron density being obtained, these
3 parameters needed to correct for shot-to-shot fluctuations and matrix effects. It must be noted,
4 however, that these issues are not an intrinsic limitation of the LIBS analytical technique.
5 Accurate Mg/Ca molar ratios (and therefore seawater temperature reconstructions) should be
6 obtainable using the aforementioned calibration-free techniques and different LIBS
7 instrumentation (i.e. an echelle-based spectrometer with higher resolution and wider
8 wavelength span).

10 3. Results

11 Fig. 3 shows two representative LIBS spectra obtained from a *P. vulgata* biogenic calcium
12 carbonate shell, for both the wide (left) and narrow (right) spectral windows. The selected LIBS
13 emission lines for Mg and Ca are highlighted in the figure.



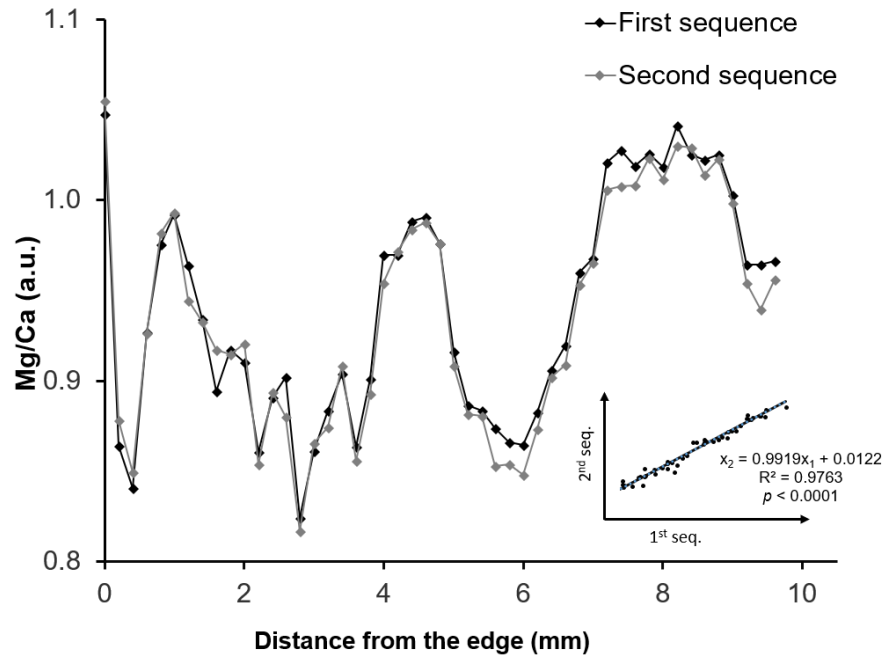
16 Fig. 3: Representative LIBS spectra of *P. vulgata* biogenic calcium carbonate using the wide spectral window (left) and the
17 narrow one (right). Analytical lines for Mg and Ca were selected based on similar intensity and close wavelengths, not
18 saturated, and free from self-absorption.

19
20 From the averaged raw (a.u.) ratio between the Mg and Ca emission line intensities measured
21 at each sampling point, an intra-mollusc shell Mg/Ca profile is plotted to show the relative
22 variation of the Mg amount along the sampling path. All the experiments showed a significant
23 fluctuation of Mg/Ca ratios along the profiles generated for each *P. vulgata* specimen. Two
24 consecutive Mg/Ca profiles were performed along the same sampling path for one specimen
25 (MA.101.3), using identical LIBS setup and experimental conditions, as shown in Fig. 4. There
26 is a substantial correlation ($R^2 = 0.98$) between the two consecutively measured Mg/Ca profiles,

1 suggesting that the LIBS measurements are highly repetitive, provided that the LIBS set-up
2 and experimental conditions are identical.

3

4



5

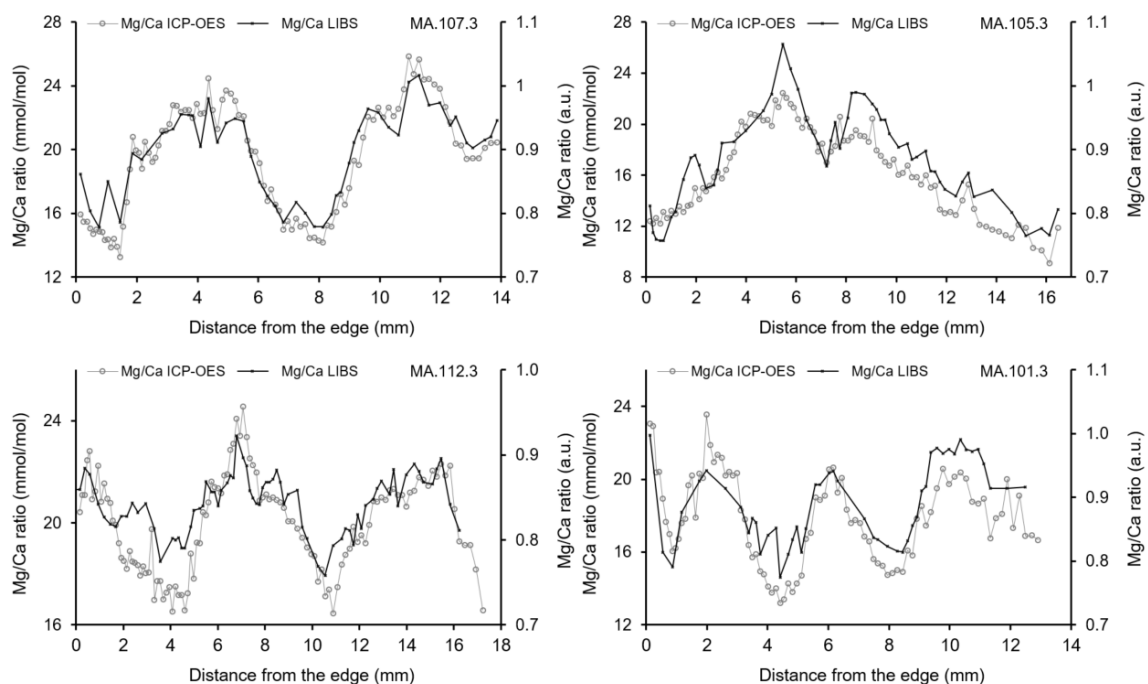
6 Fig. 4: Comparison between two consecutively measured LIBS Mg/Ca profiles measured along the same sampling path on *P.*
7 *vulgata* specimen MA.101.3. The inset shows the correlation between both sequences.

8

9 The first set of LIBS measurements obtained Mg/Ca profiles along transects from the *P.*
10 *vulgata* shell edges to each shell apex, following a sampling path along the centre of the long
11 calcite layer $m+2$ (Fig. 1). A total of 48, 57, 78 and 49 measurement points were completed at
12 a spacing of 0.2 mm on *P. vulgata* specimens MA.107.3, MA.105.3, MA.112.3 and MA.101.3,
13 respectively. LIBS-derived Mg/Ca profiles through individual shell growth series identified
14 between one and three cycles in Mg/Ca, which mimic intra-annual cycles in seawater
15 temperature (Fig. 5). The minima in LIBS Mg/Ca (0.78, 0.76, 0.77 and 0.77 a.u.) were similar
16 in all four specimens, whereas the maxima (1.04, 1.07, 1.13 and 1.00 a.u.) exhibited some
17 variability, the latter causing differences in the ranges of LIBS derived Mg/Ca (0.26, 0.31, 0.36
18 and 0.22 a.u.).

19 These LIBS Mg/Ca profiles can be compared directly with the ICP-OES Mg/Ca measurements.
20 A total of 100, 90, 115 and 88 calcite powder samples were milled from the same *P. vulgata*

1 specimens MA.107.3, MA.105.3, MA.112.3 and MA.101.3, respectively, with actual molar
 2 Mg/Ca ratios determined by comparison of ICP-OES spectral line intensities with synthetic
 3 calibration solutions, as described above. The results obtained (Fig. 5) also exhibited between
 4 one and three cycles in Mg/Ca within individual *P. vulgata* shells. The maximum Mg/Ca
 5 (25.85, 22.46, 24.56 and 23.55 mmol/mol) were more similar between specimens than the
 6 minima (13.27, 9.08, 16.45 and 13.19 mmol/mol). Therefore, the range in ICP-OES derived
 7 Mg/Ca ratios within individual *P. vulgata* specimens also exhibited some variability (12.58,
 8 13.37, 8.11 and 10.35 mmol/mol).



9

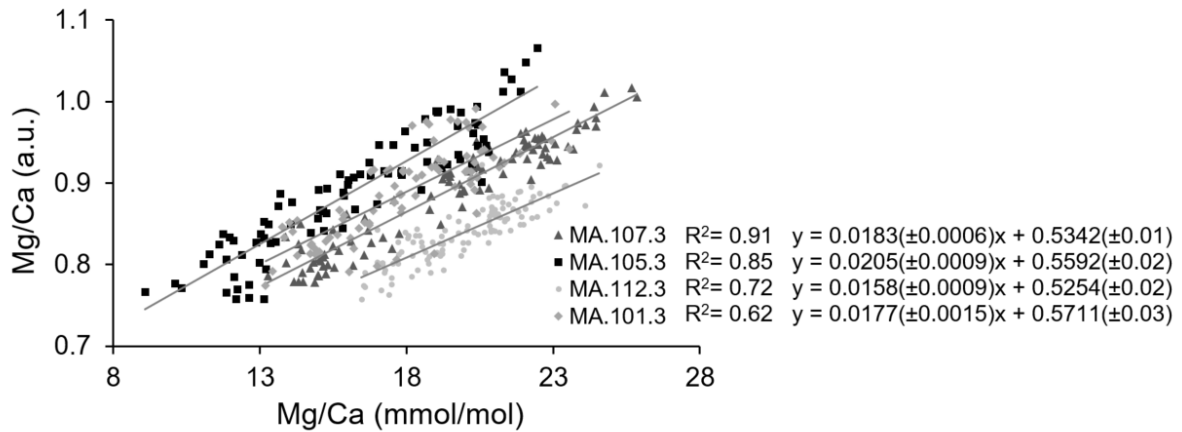
10 Fig. 5: Comparison of Mg/Ca profiles obtained by ICP-OES (open symbols and grey line) and LIBS (filled symbols and black
 11 line) for *P. vulgata* marine mollusc shell samples MA.107.2, MA.105.3, MA.112.3 and MA.101.3.

12

13 Significantly, the Mg/Ca profiles obtained by the two analytical methodologies were similar in
 14 all samples, exhibiting high correlation coefficients (Fig. 6). Both LIBS and ICP-OES
 15 techniques showed similar relative trends in Mg/Ca and also identify the same number of
 16 Mg/Ca cycles within individual *P. vulgata* specimens, these cycles interpreted here as being
 17 caused by seasonal changes in seawater temperature. However, it can be seen in Fig. 6 that
 18 there are differences in the linear regression parameters (when comparing LIBS Mg/Ca (a.u.)
 19 with ICP-OES (mmol/mol) between the four *P. vulgata* shells, which can best be attributed to

1 inconsistent LIBS experimental conditions that affect the raw LIBS Mg/Ca values, as discussed
2 in section 2.

3



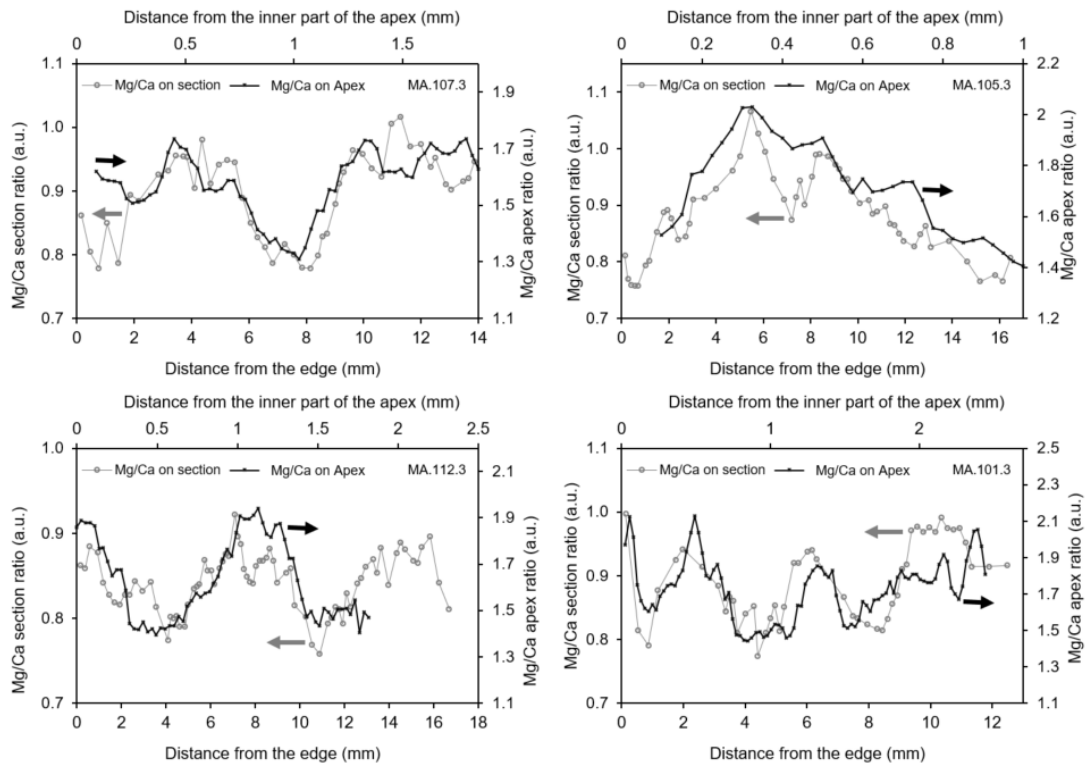
4

5 Fig. 6: Linear least squares regression between LIBS (y-axis) and ICP-OES (x-axis) Mg/Ca measurements for each *P. vulgata*
6 specimen.

7

8 The second set of LIBS measurements were performed along a shorter sampling path, close to
9 the apex of the *P. vulgata* shells that crosses the *m-2* calcite layer. Fig. 7 shows the Mg/Ca
10 profiles measured in the shell apex area compared with those generated for the longer profiles
11 through the *m+2* layer. A total of 63, 35, 66 and 96 LIBS measurement points were performed
12 at 25 μm intervals on the same *P. vulgata* specimens MA.107.3, MA.105.3, MA.112.3 and
13 MA.101.3, respectively. The number of Mg/Ca cycles identified within these shell apex
14 profiles are between one and three. The minima in LIBS apex Mg/Ca (1.31, 1.37, 1.39 and 1.44
15 a.u.) were similar in all four specimens, whereas the maxima (1.73, 2.03, 1.94 and 2.13 a.u.)
16 exhibited higher variability. Therefore, Mg/Ca ranges were 0.42, 0.66, 0.55 and 0.69 a.u. for
17 specimens MA.107.3, MA.105.3, MA.112.3 and MA.101.3, respectively.

18



1

2 Fig. 7: Comparison of Mg/Ca profiles obtained by LIBS in the $m-2$ calcite layer near the apex of the shell and by LIBS in the
 3 $m+2$ calcite layer, for samples MA.107.2, MA.105.3, MA.112.3 and MA.101.3. Note: the apex distance axis has been subject
 4 to a fixed linear stretch to facilitate visual comparison of those Mg/Ca profiles with the $m+2$ layer Mg/Ca profiles.

5 It must be noted that the absolute LIBS-determined Mg/Ca values are different between both
 6 sets of measurements, due to the second set (within the shell apex $m-2$ layer) being made with
 7 the narrow spectral window, whereas the first set (transects through the shell $m+2$ layer) was
 8 completed with the wide spectral window. Because it is not possible at present to convert the
 9 LIBS Mg/Ca ratios into mmol/mol concentration units, only relative variation (minima,
 10 maxima and cycles) of Mg/Ca can be compared. As shown in Fig. 7, the relative variation of
 11 Mg/Ca within individual specimens in similar in both areas of the *P. vulgata* shells that were
 12 sampled, for all four specimens, confirming that measurement of Mg/Ca in the shell apex
 13 region is an appropriate sampling approach.

14

15 4. Discussion

16

17 4.1 Comparison of techniques: LIBS vs ICP-OES determined intra-shell Mg/Ca profiles

1 Because LIBS offers some advantages (i.e. primarily speed of analysis) over the established
2 ICP-based techniques for the determination of elemental ratios in marine mollusc carbonate
3 shells, there is interest in assessing LIBS performance for such applications. Fig. 5 illustrates
4 very high similarity between the LIBS and ICP-OES Mg/Ca determinations within the same
5 calcite layer of archaeological *P. vulgata* shells. Any small differences between the two
6 techniques can most likely be attributed to two different reasons. First, the intrinsic lower
7 precision of LIBS due to the shot-to-shot plasma variability [34]. However, Fig. 4 indicates
8 that LIBS has potential to generate highly repetitive Mg/Ca profiles, albeit only when LIBS
9 operating conditions are consistent and probably only when shell Mg concentrations are high
10 enough (which is not the case for all marine mollusc species). Second, the two analytical
11 techniques do actually sample slightly different parts of the *P. vulgata* shells. For ICP-OES
12 Mg/Ca determinations, powder material is extracted by micromilling the complete sectioned
13 width of individual contemporaneously-deposited shell growth increments that stretch the
14 complete thickness of the calcite layer, with a total carbonate mass of more than 100 μg for
15 each sampled point. In contrast, LIBS laser pulses produce craters 100 μm in diameter with an
16 ablated mass of carbonate of only ca. 0.2 μg (500 times lower than that measured by ICP-OES).
17 This reduction in both the quantity of CaCO_3 and cross-section area sampled by LIBS
18 potentially facilitates detection of smaller scale variations in magnesium incorporated within
19 individual shell growth increments. Other studies have shown that growth lines (separating
20 shell growth increments) can contain more organic material and a higher amount of Mg [35]
21 which could produce a sudden increase in Mg/Ca, unrelated to ambient seawater temperature
22 variations, when these growth lines are sampled. For those laser-based analytical techniques
23 that only sample small areas within growth increments (i.e. LIBS and LA-ICP-MS), these
24 observations suggest that an alternative sampling strategy, other than a simple path along the
25 centre of the calcite $m+2$ layer, should be used. A previous work by Hausmann et al has
26 explored a 2D grid sampling of the complete calcite layer of other kind of shells, but the results,
27 showing annual trends as well as local heterogeneities, are difficult to validate against other
28 analytical techniques [11].

29

30 Other studies have proposed that magnesium concentrations are heterogeneous within
31 individual contemporaneously-deposited growth increments [11].

1 In any case, further studies are required in order to investigate the spatial heterogeneity of
2 elemental incorporation within contemporaneous shell growth increments, and such
3 investigations should be undertaken for all marine mollusc species that might be used as
4 archives of past climate change (including seawater temperature variability). Due to the smaller
5 sampling volumes and the higher spatial resolution achievable using LIBS, as well as its lower
6 cost than LA-ICP-MS, this analytical technique possibly can offer new insights on magnesium
7 incorporation into different parts of marine mollusc shells.

9 **4.2 LIBS Mg/Ca profiles measured in the *P. vulgata* shell apex area**

10 Elemental ratios in *P. vulgata* marine mollusc shells are typically measured in the calcite $m+2$
11 shell layer [9, 36, 37], because that part of the shell covers most of the mollusc's lifespan with
12 high shell deposition rates, resulting in a long section that enables high temporal resolution
13 measurements. The $m-2$ calcite layer located near the *P. vulgata* shell apex is now shown to
14 preserve the same Mg/Ca record [25], but is compressed into a thickness of only a few
15 millimetres. Therefore, powder micromilling techniques cannot achieve sampling at high
16 enough spatial (and thus temporal) resolution within this shell apex area. Only one study [30]
17 has measured elemental ratios in the *Patella* shell apex, applying LA-ICP-MS to modern *P.*
18 *vulgata* shells. Although those results showed cycles (presumably seasonal) in Mg/Ca, those
19 cycles were not correlated with other Mg/Ca profiles generated in other shell layers, nor were
20 correlated with other techniques or with ambient seawater temperature.

21 This study shows a high similarity between LIBS Mg/Ca profiles measured in the apex $m-2$
22 shell layer and Mg/Ca profiles generated for the thicker $m+2$ shell layer. One advantage of
23 generating Mg/Ca profiles within the shell apex area is that the high spatial resolution
24 achievable using LIBS and the speed of this technique could lead to faster generation of Mg/Ca
25 profiles with a sufficient number of data points to maintain high temporal resolution and
26 capture intra-annual changes within Mg/Ca profiles. Perhaps more importantly, because the
27 growth increments in the shell apex are aligned parallel to the interior edge of the shell,
28 measurements can be performed using LIBS depth profiling from the exterior *P. vulgata* shell
29 surface [38], removing the requirement to section shell specimens or undertake any other time
30 consuming sample preparation.

1 **4.3 Archaeological applications**

2 Mg/Ca profiles within archaeological shells recovered from shell middens could be used for
3 season-of-capture investigations, i.e. assessment of when this marine food resource was
4 harvested by prehistoric societies. Such applications must assume that cycles in Mg/Ca within
5 individual marine mollusc shells are following intra-annual (i.e. seasonal changes) in seawater
6 temperature, with high Mg/Ca correlating with the warmest (summer) months and low Mg/Ca
7 correlating with the coldest (winter) months [9, 39]. However, it must also be recognised that
8 cessation of mollusc shell growth might also occur during the coldest and hottest times of the
9 year [29, 36], such that shell-derived Mg/Ca time series do not capture the full 12 months of
10 ambient seawater temperature.

11 For season-of-capture studies to be undertaken Mg/Ca profiles do not need to be generated for
12 an entire marine mollusc shell thickness. Rather, it is sufficient to be able to identify trends in
13 the Mg/Ca records nearest to the shell edges (i.e. the most recently deposited shell material),
14 as well as by comparison with the proximal maximum or minimum in Mg/Ca. Following such
15 an approach, interpretation of Fig. 5 shows that the season-of-capture of the four archaeological
16 *P. vulgata* specimens investigated in this study is spring, winter, autumn and summer for
17 MA.107.2, MA.105.3, MA.112.3 and MA.101.3, respectively.

18

19 It must be noted that for these archaeological studies only the relative intra-shell variation of
20 the Mg/Ca ratio is needed. Therefore, the limitation of our current instrumental setup to obtain
21 quantitative values (due to the low resolution and low number of available analytical lines)
22 does not preclude its application. Even with this limitation, LIBS offers fast measurement time,
23 considerably reduced sample preparation time (potentially even none, if LIBS depth profiling
24 from the exterior shell surface is applied) and low cost of instrumentation. Specifically, the
25 advantages that LIBS offers for archaeological studies are an approximately 20x reduction in
26 time required to measure an individual *P. vulgata* specimen (ca. 1 hour is required to measure
27 and process LIBS spectral information per shell sample, compared to ca. 20 hours to micromill
28 calcium carbonate powders and to prepare sample solutions for ICP-OES, as well as subsequent
29 processing of emission intensity data). Although spatially-resolved elemental measurements,
30 including within marine mollusc shells, can be undertaken using LA-ICP-MS, that is much
31 more costly and complex analytical instrumentation.

32 **5. Conclusions**

1 This study presents comparative analysis of Mg/Ca profiles measured within shells of
2 archaeological specimens of the common limpet *P. vulgata*, using ICP-OES and LIBS
3 analytical techniques. The results validate application of the LIBS analytical technique for this
4 application; LIBS has rarely been applied to marine mollusc shells, but this analytical technique
5 can offer several distinct advantages over conventional spectrometry techniques (ICP-OES,
6 ICP-MS and LA-ICP-MS), including faster measurements, minimal (or potentially even no)
7 sample preparation, easy automation and less complex and lower cost instrumentation.

8 Mg/Ca profiles measured in the $m+2$ calcite layer of sectioned specimens of four
9 archaeological *P. vulgata* shells using LIBS and ICP-OES are highly correlated (R^2 values from
10 0.62 to 0.91). Both analytical techniques record the same cycles in Mg/Ca within individual *P.*
11 *vulgata* shells, interpreted to represent intra-annual (seasonal) changes in seawater temperature.
12 LIBS Mg/Ca profiles have also been generated, for the first time, in the *P. vulgata* $m-2$ calcite
13 layer near the shell apex. The shell apex Mg/Ca profiles exhibit a high degree of similarity with
14 the Mg/Ca profiles that are more traditionally generated for the $m+2$ calcite layer. Because of
15 the nature and orientation of incremental shell growth within the *P. vulgata* shell apex region,
16 there is the possibility of applying the LIBS depth profiling technique to the shell apex to
17 generate Mg/Ca profiles, without the need for any shell specimen preparation (i.e. sectioning).

18 The now proven utility of the LIBS analytical technique for robust generation of Mg/Ca
19 profiles within *P. vulgata* shells has significant implications for archaeological studies. LIBS
20 will allow much faster generation of *P. vulgata* shell Mg/Ca profiles (a ca. 20-fold reduction
21 in sample preparation and measurement time cf. ICP-OES). Consequently, the number of
22 mollusc shell specimens collected from any archaeological site, as well as from any
23 chronological level within any archaeological site, that can be subject to determination of intra-
24 shell Mg/Ca profiles will be considerably increased using the LIBS analytical technique,
25 thereby improving the statistical significance of datasets and robustness of interpretations. One
26 example archaeological application that will benefit from LIBS Mg/Ca profiles is season-of-
27 capture of marine mollusc as a food resource for the prehistoric societies.

28 Future research will focus on development of the LIBS depth-profiling technique for
29 generation of intra-shell Mg/Ca profiles, primarily to remove the requirement for sectioning of
30 mollusc shell specimens, as well as the use of calibration-free LIBS techniques (using a
31 different instrumental setup, specifically, a multichannel compact CCD spectrometer with high
32 resolution and wide wavelength span) so that actual molar Mg/Ca (i.e. as mmol/mol) profiles

1 can be generated. Quantitative determination of Mg/Ca profiles for a large number of modern
2 shell specimens, with known contemporaneous seawater temperatures during shell formation,
3 will potentially facilitate robust calibration of the Mg/Ca vs. seawater temperature dependence
4 for different marine mollusc species, thereby enabling more precise paleoclimatic studies.

7 **Acknowledgments**

8 This research was performed as part of the projects “TRACECHANGE: Tracing Climatic
9 Abrupt Change Events and its Social Impact during the Late Pleistocene and Early Holocene
10 (15-7 ky cal BP) (HAR2013-46802-P)”, and “Photonics Sensors for Safety & Security
11 (SENSA)” (TEC2016-76021-C2-2-R), both funded by the Spanish Ministry of Economy and
12 Competitiveness. A. García-Escárczaga’s work was funded by the University of Cantabria
13 through a predoctoral grant and I. Gutiérrez-Zugasti’s work was funded by the Spanish
14 Ministry of Economy and Competitiveness through a Juan de la Cierva grant (grant JCI-2012-
15 12094). We thank Universidad de Cantabria (UC), Manchester Metropolitan University
16 (MMU), Universidad Complutense de Madrid (UCM), Instituto Internacional de
17 Investigaciones Prehistóricas de Cantabria (IIIPC) and Grupo de Ingeniería Fotónica (GIF) for
18 providing support. We would also like to thank David Cuenca-Solana (IIIPC), Javier Martín-
19 Chivelet (UCM), Lucia Agudo Pérez (IIIPC), David McKendry (MMU), and Luis Rodríguez-
20 Cobo (GIF) for their expertise and input to this study.

22 **References**

- 24 [1] J. Veizer, A. Prokoph, Temperatures and oxygen isotopic composition of Phanerozoic oceans, *Earth-*
25 *Science Reviews*, 146 (2015) 92-104.
26 [2] I. Gutiérrez-Zugasti, S.H. Andersen, A.C. Araújo, C. Dupont, N. Milner, A.M. Monge-Soares, Shell
27 midden research in Atlantic Europe: State of the art, research problems and perspectives for the
28 future, *Quaternary International*, 239 (2011) 70-85.
29 [3] N. Hallmann, M. Burchell, B.R. Schöne, G.V. Irvine, D. Maxwell, High-resolution sclerochronological
30 analysis of the bivalve mollusk *Saxidomus gigantea* from Alaska and British Columbia: techniques for
31 revealing environmental archives and archaeological seasonality, *Journal of Archaeological Science*,
32 36 (2009) 2353-2364.

- 1 [4] L.-L. Cui, X. Wang, Determination of carbon and oxygen isotopes of geological samples with a
2 complicated matrix: comparison of different analytical methods, *Analytical Methods*, 6 (2014) 9173-
3 9178.
4
- 5 [6] S.R. Durham, D.P. Gillikin, D.H. Goodwin, G.P. Dietl, Rapid determination of oyster lifespans and
6 growth rates using LA-ICP-MS line scans of shell Mg/Ca ratios, *Palaeogeography, Palaeoclimatology,*
7 *Palaeoecology*, (2017).
- 8 [7] L. Bougeois, M. de Rafélis, G.-J. Reichart, L. de Nooijer, G. Dupont-Nivet, Using Mg/Ca on oyster
9 shells as paleoclimatic proxy, example from the Paleogene of Central Asia, in: *EGU General Assembly*
10 *Conference Abstracts*, 2015, pp. 493.
- 11 [8] B.R. Schöne, Z. Zhang, P. Radermacher, J. Thébault, D.E. Jacob, E.V. Nunn, A.-F. Maurer, Sr/Ca and
12 Mg/Ca ratios of ontogenetically old, long-lived bivalve shells (*Arctica islandica*) and their function as
13 paleotemperature proxies, *Palaeogeography, Palaeoclimatology, Palaeoecology*, 302 (2011) 52-64.
- 14 [9] A. Cobo, A. García-escárzaga, I. Gutiérrez Zugasti, J. Setien-Marquinez, M.R. González-orales, J.M.
15 Higuera, Automated measurement of Magnesium/Calcium ratios in gastropod shells using Laser-
16 Induced Breakdown Spectroscopy (LIBS) for paleoclimatic applications, *Applied Spectroscopy*, 71
17 (2017) 1-9.
- 18 [10] A. García-Escárzaga, S. Moncayo, I. Gutiérrez-Zugasti, M.R. González-Morales, J. Martín-Chivelet,
19 J. Cáceres, Mg/Ca ratios measured by laser induced breakdown spectroscopy (LIBS): a new approach
20 to decipher environmental conditions, *Journal of Analytical Atomic Spectrometry*, 30 (2015) 1913-
21 1919.
- 22 [11] N. Hausmann, P. Siozos, A. Lemonis, A.C. Colonese, H.K. Robson, D. Anglos, Elemental mapping of
23 Mg/Ca intensity ratios in marine mollusc shells using laser-induced breakdown spectroscopy, *Journal*
24 *of Analytical Atomic Spectrometry*, (2017).
- 25 [12] C.A. Akpovo, J.A. Martinez Jr, D.E. Lewis, J. Branch, A. Schroeder, M.D. Edington, L. Johnson,
26 Regional discrimination of oysters using laser-induced breakdown spectroscopy, *Analytical Methods*,
27 5 (2013) 3956-3964.
- 28 [13] S.J. Rehse, N. Jeyasingham, J. Diedrich, S. Palchadhuri, A membrane basis for bacterial
29 identification and discrimination using laser-induced breakdown spectroscopy, *Journal of Applied*
30 *Physics*, 105 (2009) 102034.
- 31 [14] B.E. Naes, S. Umpierrez, S. Ryland, C. Barnett, J.R. Almirall, A comparison of laser ablation
32 inductively coupled plasma mass spectrometry, micro X-ray fluorescence spectroscopy, and laser
33 induced breakdown spectroscopy for the discrimination of automotive glass, *Spectrochimica Acta Part*
34 *B: Atomic Spectroscopy*, 63 (2008) 1145-1150.
- 35 [15] J.D. Winefordner, I.B. Gornushkin, T. Correll, E. Gibb, B.W. Smith, N. Omenetto, Comparing several
36 atomic spectrometric methods to the super stars: special emphasis on laser induced breakdown
37 spectrometry, LIBS, a future super star, *Journal of Analytical Atomic Spectrometry*, 19 (2004) 1061-
38 1083.
- 39 [16] P. Freitas, L.J. Clarke, H. Kennedy, C. Richardson, F. Abrantes, Mg/Ca, Sr/Ca, and stable-isotope
40 ($\delta^{18}\text{O}$ and $\delta^{13}\text{C}$) ratio profiles from the fan mussel *Pinna nobilis*: Seasonal records and temperature
41 relationships, *Geochemistry, Geophysics, Geosystems*, 6 (2005) n/a-n/a.
- 42 [17] P.S. Freitas, L.J. Clarke, H. Kennedy, C.A. Richardson, The potential of combined Mg/Ca and $\delta^{18}\text{O}$
43 measurements within the shell of the bivalve *Pecten maximus* to estimate seawater $\delta^{18}\text{O}$
44 composition, *Chemical Geology*, 291 (2012) 286-293.
- 45 [18] V. Mouchi, M. De Rafélis, F. Lartaud, M. Fialin, E. Verrecchia, Chemical labelling of oyster shells
46 used for time-calibrated high-resolution Mg/ca ratios: A tool for estimation of past seasonal
47 temperature variations, *Palaeogeography, Palaeoclimatology, Palaeoecology*, 373 (2013) 66-74.
- 48 [19] S. Sosdian, D.K. Gentry, C.H. Lear, E.L. Grossman, D. Hicks, Y. Rosenthal, Strontium to calcium
49 ratios in the marine gastropod *Conus ermineus*: Growth rate effects and temperature calibration,
50 *Geochemistry, Geophysics, Geosystems*, 7 (2006).

- 1 [20] L. Graniero, D. Surge, D. Gillikin, I.B. i Godino, M. Álvarez, Assessing elemental ratios as a
2 paleotemperature proxy in the calcite shells of patelloid limpets, *Palaeogeography,*
3 *Palaeoclimatology, Palaeoecology*, 465 (2017) 376-385.
- 4 [21] M. Pena-Icart, M.S. Pomares-Alfonso, F.W. Batista de Aquino, C. Alonso-Hernandez, Y. Bolanos-
5 Alvarez, E.R. Pereira-Filho, Fast and direct detection of metal accumulation in marine sediments using
6 laser-induced breakdown spectroscopy (LIBS): a case study from the Bay of Cienfuegos, Cuba[dagger],
7 *Analytical Methods*, 9 (2017) 3713-3719.
- 8 [22] I. Gutiérrez-Zugasti, Coastal resource intensification across the Pleistocene–Holocene transition
9 in Northern Spain: Evidence from shell size and age distributions of marine gastropods, *Quaternary*
10 *International*, 244 (2011) 54-66.
- 11 [24] I. Gutiérrez Zugasti, D. Cuenca Solana, Biostratigraphy of shells and climate changes in the
12 Cantabrian region (northern Spain) during the Pleistocene-Holocene transition, in: K. Szabó, C.
13 Dupont, V. Dimitrijevic, L. Gómez-Castélum, N. Serrand (Eds.) *Archaeomalacology Shells in the*
14 *Arcaheological Record*, British Archaeological Reports International Series, Oxford, 2014, pp. 225-234
- 15
- 16 [25] T. Fenger, D. Surge, B. Schöne, N. Milner, Sclerochronology and geochemical variation in limpet
17 shells (*Patella vulgata*): A new archive to reconstruct coastal sea surface temperature, *Geochemistry,*
18 *Geophysics, Geosystems*, 8 (2007).
- 19 [26] S. de Villiers, M. Greaves, H. Elderfield, An intensity ratio calibration method for the accurate
20 determination of Mg/Ca and Sr/Ca of marine carbonates by ICP-AES, *Geochemistry, Geophysics,*
21 *Geosystems*, 3 (2002).
- 22 [27] M. Greaves, S. Barker, C. Daunt, H. Elderfield, Accuracy, standardization, and interlaboratory
23 calibration standards for foraminiferal Mg/Ca thermometry, *Geochemistry, Geophysics, Geosystems,*
24 6 (2005).
- 25 [28] M. Greaves, N. Caillon, H. Rebaubier, G. Bartoli, S. Bohaty, I. Cacho, L. Clarke, M. Cooper, C. Daunt,
26 M. Delaney, Interlaboratory comparison study of calibration standards for foraminiferal Mg/Ca
27 thermometry, *Geochemistry, Geophysics, Geosystems*, 9 (2008).
- 28 [29] I. Gutiérrez-Zugasti, R. Suárez-Revilla, L.J. Clarke, B.R. Schöne, G.N. Bailey, M.R. González-Morales,
29 Shell oxygen isotope values and sclerochronology of the limpet *Patella vulgata* Linnaeus 1758 from
30 northern Iberia: Implications for the reconstruction of past seawater temperatures, *Palaeogeography,*
31 *Palaeoclimatology, Palaeoecology*, 475 (2017) 162-175.
- 32 [30] W.G. Ambrose, W.L. Locke V, G.F. Bigelow, P.E. Renaud, Deposition of annual growth lines in the
33 apex of the common limpet (*Patella vulgata*) from Shetland Islands, UK and Norway: Evidence from
34 field marking and shell mineral content of annual line deposition, *Environmental Archaeology*, 21
35 (2016) 79-87.
- 36 [31] W.B. Barnett, V.A. Fassel, R.N. Kniseley, Theoretical principles of internal standardization in
37 analytical emission spectroscopy, *Spectrochimica Acta Part B: Atomic Spectroscopy*, 23 (1968) 643-
38 664.
- 39 [32] D.W. Hahn, N. Omenetto, Laser-Induced Breakdown Spectroscopy (LIBS), Part II: Review of
40 Instrumental and Methodological Approaches to Material Analysis and Applications to Different
41 Fields, *Applied Spectroscopy*, 66 (2012) 347-419.
- 42 [33] E. Tognoni, G. Cristoforetti, S. Legnaioli, V. Palleschi, Calibration-Free Laser-Induced Breakdown
43 Spectroscopy: State of the art, *Spectrochimica Acta Part B: Atomic Spectroscopy*, 65 (2010) 1-14.
- 44 [34] A.P. Michel, A.D. Chave, Analysis of laser-induced breakdown spectroscopy spectra: the case for
45 extreme value statistics, *Spectrochimica Acta Part B: Atomic Spectroscopy*, 62 (2007) 1370-1378.
- 46 [35] B.R. Schöne, Z. Zhang, D. Jacob, D.P. Gillikin, T. Tütken, D. Garbe-Schönberg, A. SOLDATI, Effect of
47 organic matrices on the determination of the trace element chemistry (Mg, Sr, Mg/Ca, Sr/Ca) of
48 aragonitic bivalve shells (*Arctica islandica*)—Comparison of ICP-OES and LA-ICP-MS data, *Geochemical*
49 *journal*, 44 (2010) 23-37.

1 [36] D. Surge, T. Wang, I. Gutierrez-Zugasti, P.H. Kelley, Isotope sclerochronology and season of annual
2 growth line formation in limpet shells (*Patella vulgata*) from cold- and warm-temperate zones in the
3 eastern North Atlantic, *PALAIOS*, 28 (2013) 386-393.

4 [37] A. García-Escárzaga, I. Gutiérrez-Zugasti, M.R. González-Morales, A. Cobo, Shells and Humans:
5 Molluscs and Other Coastal Resources from the Earliest Human Occupations at the Mesolithic Shell
6 Midden of El Mazo (Asturias, Northern Spain) *Papers from the Institute of Archaeology*, 27 (2017) Art.
7 3.

8 [38] R. Cerrato, A. Casal, M.P. Mateo, G. Nicolas, Dealloying evidence on corroded brass by laser-
9 induced breakdown spectroscopy mapping and depth profiling measurements, *Spectrochimica Acta*
10 *Part B: Atomic Spectroscopy*, 130 (2017) 1-6.

11 [39] J.E. Ferguson, G.M. Henderson, D.A. Fa, J.C. Finlayson, N.R. Charnley, Increased seasonality in the
12 Western Mediterranean during the last glacial from limpet shell geochemistry, *Earth and Planetary*
13 *Science Letters*, 308 (2011) 325-333.

14